Identification of Genes Selectively Regulated by IFNs in Endothelial Cells[1]

Stefano Indraccolo,* Ulrich Pfeffer,† Sonia Minuzzo,‡ Giovanni Esposito,* Valeria Roni,§ Susanna Mandruzzato,‡ Nicoletta Ferrari,† Luca Anfosso,†¶ Raffaella Dell'Eva,† Douglas M. Noonan,¶ Luigi Chieco-Bianchi,‡ Adriana Albini,2∥ and Alberto Amadori2,3*‡

IFNs are highly pleiotropic cytokines also endowed with marked antiangiogenic activity. In this study, the mRNA expression profiles of endothelial cells (EC) exposed in vitro to IFN-α, IFN-β, or IFN-γ were determined. We found that in HUVEC as well as in other EC types 175 genes were up-regulated (>2-fold increase) by IFNs, including genes involved in the host response to RNA viruses, inflammation, and apoptosis. Interestingly, 41 genes showed a >5-fold higher induction by IFN-α in EC compared with human fibroblasts; among them, the gene encoding the angiostatic chemokine *CXCL11* was selectively induced by IFN-α in EC along with other genes associated with angiogenesis regulation, including *CXCL10*, *TRAIL*, and *guanylate-binding protein 1*. These transcriptional changes were confirmed and extended by quantitative PCR analysis and ELISA; whereas IFN-α and IFN-β exerted virtually identical effects on transcriptome modulation, a differential gene regulation by type I and type II IFN emerged, especially as far as quantitative aspects were concerned. In vivo, IFN-α-producing tumors overexpressed murine CXCL10 and CXCL11, guanylate-binding protein 1, and TRAIL, with evidence of CXCL11 production by tumor-associated EC. Overall, these findings improve our understanding of the antiangiogenic effects of IFNs by showing that these cytokines trigger an antiangiogenic transcriptional program in EC. Moreover, we suggest that quantitative differences in the magnitude of the transcriptional activation of IFN-responsive genes could form the basis for cell-specific transcriptional signatures.   *The Journal of Immunology,* 2007, 178: 1122–1135.

Interferon-α is a potent cytokine endowed with remarkable antiangiogenic activity that was first noticed many years ago (1) and subsequently confirmed in different tumor models (2–4). This activity has been mainly attributed to indirect effects, including inhibition of basic fibroblast growth factor production by tumor cells (5) or down-regulation of IL-8 and vascular endothelial growth factor gene expression (6, 7). In contrast, other data indicate that IFN-α also has direct effects on endothelial cells (EC),[4]

including impairment of EC proliferation and migration (3, 4, 8). In addition, IFN-γ may exert antiangiogenic activity both directly through cytostatic effects on proliferating EC (9) and indirectly through the induction of angiostatic chemokine expression in vivo (10, 11).

To date, the gene expression profile induced by IFN-α has been predominantly studied in tumor cell lines (12–14) and some primary cells, including PBMC, T lymphocytes, and dendritic cells (15–18); little is known about the transcriptional profile induced by IFN-α in EC. The definition of cell type-specific profiles is likely central to a full understanding of the biology of IFNs and their antiangiogenic activity and may also be of potential clinical importance given the broad use of these cytokines in patients. To investigate this matter, we pulsed in vitro human and murine EC of different anatomical origin and differentiation status with human rIFN-α, rIFN-β, or rIFN-γ and analyzed their gene expression profile using microarrays. The results presented here represent the most comprehensive analysis of gene expression regulated by IFNs in human EC currently available.

Materials and Methods

Cell lines and in vitro culture

HUVEC were isolated from freshly obtained umbilical cord samples by collagenase digestion of the umbilical vein (19). Primary cultures were serially split in flasks coated with collagen type I (10 μg/cm^2; Sigma-Aldrich) and maintained in TC 199 medium supplemented with 20% FCS (Invitrogen Life Technologies), human rβ-EC growth factor (0.1 ng/ml; Sigma-Aldrich), human recombinant basic fibroblast growth factor (10 ng/ml; Peprotech), and heparin (50 μg/ml). Human primary fibroblasts (HF) were obtained by mechanical disruption of the connective tissue of the umbilical cord and cultured in DMEM (Sigma-Aldrich) supplemented with 10% FCS and 2 mM L-glutamine. Primary cultures of human dermal microvascular endothelial cells (HMVEC) were purchased from Cascade Biologics and maintained in M131 medium supplemented with microvascular growth supplement (Cascade Biologics). Primary cells were used between

*Istituto Oncologico Veneto, Padua, Italy; †Istituto Nazionale per la Ricerca sul Cancro, Genoa, Italy; ‡Department of Oncology and Surgical Sciences, University of Padua, Padua, Italy; §Department of Molecular Genetics, University Eye Hospital, Tuebingen, Germany; ¶Department of Clinical and Biological Sciences, University of Insubria, Varese, Italy; and ∥Istituto di Ricovero e Cura a Carattere Scientifico MultiMedica, Milan, Italy

[2] A. A. and A. A. contributed equally to this study

[3] Address correspondence and reprint requests to Dr. Alberto Amadori, Department of Oncology and Surgical Sciences, University of Padua, Via Gattamelata, 64, I-35128 Padua, Italy. E-mail address: albido@unipd.it

[4] Abbreviations used in this paper: EC, endothelial cell; GBP, guanylate-binding protein; HF, human primary fibroblast; HMVEC, human dermal microvascular EC; HMVAR, human renal macrovascular EC; VTH, vascular endothelial growth factor, TNF-α, and heparin.

Table I. *Sequences of primers used in quantitative RT-PCR experiments*

Primer[a]	Sequence
IFTI SN	5'-cagaacggctgcctaatttac-3'
IFTI ASN	5'-caggcatttcatcgtcatcaat-3'
CXCL11 SN	5'-cttggctgtgatattgtgtgc-3'
CXCL11 ASN	5'-gggtacattatggaggctttc-3'
CXCL10 SN	5'-cgattctgatttgctgccttat-3'
CXCL10 ASN	5'-ggcttgcaggaataatttcaagt-3'
CXCL9 SN	5'-gcatcatcttgctggttctg-3'
CXCL9 ASN	5'-taggtggatagtcccttgg-3'
MX1 SN	5'-gaagatggttgtttccgaagtg-3'
MX1 ASN	5'-ttctcctcatactggctgc-3'
GBP-1 SN	5'-aaagaatgagcagatgatggaac-3'
GBP-1 ASN	5'-gttgctcctgttcctgaag-3'
TNFSF10 SN	5'-agtctctctgtgtggctg-3'
TNFSF10 ASN	5'-gggtcccaataactgtcatc-3'
STAT1 SN	5'-catgaaatcaagagcctggaag-3'
STAT1 ASN	5'-gatcactctttgccacacc-3'
STAT2 SN	5'-tgggtgctactaccagga-3'
STAT2 ASN	5'-cagctctaatgactccagc-3'
IL-15 SN	5'-gagccaactgggtgaatg-3'
IL-15 ASN	5'-gggtgaacatcactttccg-3'
IL-12A SN	5'-gctggcagttattgatgagc-3'
IL-12A ASN	5'-gcatgaagaagtatgcagagc-3'
CX3CL1 SN	5'-gccaccttctgccatctg-3'
CX3CL1 ASN	5'-tctcgtctccaagatgattgc-3'
CCL8 SN	5'-gctggagagctacacaag-3'
CCL8 ASN	5'-gtccatgtatgaaggctcatg-3'
CASP1 SN	5'-ttgagcagccagatggtag-3'
CASP1 ASN	5'-ttattcagcagacataattcc-3'
OASL SN	5'-gaggagtttctgaggcag-3'
OASL ASN	5'-ccagctccacctctctg-3'
TP53 SN	5'-ccagccaaagaagaaaccac-3'
TP53 ASN	5'-cctcattcagctctcggaac-3'
RPII SN	5'-gacaatgcagagaagctgg-3'
RPII ASN	5'-gcaggaagacatcatcatcc-3'
GAPDH SN	5'-gaaggtgaaggtcggagt-3'
GAPDH ASN	5'-catgggtggaatcatattggaa-3'

[a] SN, Sense; ASN, antisense.

the fourth and the seventh in vitro passage. Cultures of human macrovascular EC obtained from the renal artery (HMVAR) were donated by Dr. A. Caruso (University of Brescia, Brescia, Italy) and were maintained in M131 medium. The murine 1G11 lung endothelial cell line and dermal microvascular EC of the SIEC cell line were obtained from Dr. A. Vecchi (Mario Negri Institute, Milan, Italy) and were cultured in DMEM supplemented with 20% FCS, 1 mM L-glutamine, 1% nonessential amino acids, 1 mM sodium pyruvate, EC growth supplement (Sigma-Aldrich), and heparin (100 μg/ml). The human breast cancer cell line MCF7, obtained from American Type Culture Collection, was grown in DMEM supplemented with 10% FCS and 2 mM L-glutamine; IFN-α-producing MCF7 cells were obtained by the transduction of parental MCF7 cells with a murine IFN-α-encoding retroviral vector as reported elsewhere (4).

Before processing as detailed below, human EC and HF were incubated at 37°C for 5 h in a humidified atmosphere of 5% CO_2 in air alone or in the presence of rIFN-α, rIFN-β (both purchased from Schering-Plough), or rIFN-γ (purchased from Peprotech) at 1000 IU/ml; SIEC and 1G11 cells were incubated with 1000 IU/ml murine rIFN-α (PBL Laboratories).

Preparation of RNA and cRNA

Total RNA was isolated from EC and HF cultured as above using the RNeasy Mini kit (Qiagen) according to the manufacturer's instructions. cDNA synthesis was performed using T7-(dT)$_{24}$ oligonucleotide primers and the Custom SuperScript double-stranded cDNA synthesis kit (Invitrogen Life Technologies). Double-stranded cDNA was extracted with phenol-chloroform-isoamyl alcohol (25:24:1), precipitated with ethanol, and used to prepare cRNA using the BioArray high-yield RNA transcription kit (Affymetrix) according to manufacturer's instructions. cRNA was purified using the RNeasy Mini kit as described above, controlled by agarose gel electrophoresis and RNA 6000 Pico assay (Agilent), and subjected to fragmentation for 35 min at 94°C in fragmentation buffer (40 mM Tris-acetate (pH 8.1), 100 mM CH_3COOH, and 30 mM $Mg(CH_3COO)_2 \cdot 4H_2O$).

GeneChip microarray analysis and data normalization

Labeled cRNA was used for screening of GeneChip human genome U133A arrays (Affymetrix). The experiment consisted of three biological replicates for control and IFN-treated HUVEC and two biological replicates for all the other conditions; in some cases, technical replicates were also performed. Each biological replicate consisted of four independent experiments with different donors that were pooled before hybridization. Data concerning the effects of IFN-β are based on a single biological replicate with two technical replicates. Microarray analysis of HMVEC was performed on cDNA obtained from IFN-treated or control HMVEC cultures from two different donors. Hybridization and scanning was conducted on the Affymetrix platform. Data were normalized following the GeneChip robust multiarray average (GCRMA) procedure (20) of Bioconductor 1.4 (21) (www.bioconductor.org). Statistically significant expression changes were determined using permutation tests (Significance Analysis of Microarrays (SAM); www-stat.stanford.edu/~tibs/SAM/) (22). Genes regulated at least 2-fold in comparison to untreated controls were considered. The delta value was set to return a median false significant number of <1.

Table II. *Classes of genes induced by IFN-α in HUVEC[a]*

Gene Category	List Hits	List Total	Population Hits	Population Total	EASE Score	Bonferroni
Biological process						
Immune response	65	228	272	7033	3.07E-39	8.08E-36
Defense response	66	228	296	7033	6.92E-38	1.82E-34
Response to biotic stimulus	69	228	346	7033	1.87E-36	4.94E-33
Response to external stimulus	72	228	517	7033	1.04E-27	2.73E-24
Response to pest/pathogen/parasite	29	228	166	7033	2.95E-13	7.77E-10
Inflammatory response	15	228	64	7033	1.02E-08	2.69E-05
Innate immune response	15	228	65	7033	1.26E-08	3.33E-05
Response to wounding	16	228	90	7033	1.44E-07	3.80E-04
Receptor binding	19	224	157	7079	1.84E-06	4.85E-03
Cell-cell signaling	19	228	156	7033	2.37E-06	6.25E-03
Molecular function						
Defense/immunity protein activity	18	224	58	7079	1.01E-12	2.67E-09
Antiviral response protein activity	11	224	20	7079	1.10E-10	2.91E-07
Cytokine activity	15	224	61	7079	3.82E-09	1.01E-05
Chemokine activity	6	224	13	7079	3.11E-05	8.18E-02
Chemoattractant activity	6	224	13	7079	3.11E-05	8.18E-02
G protein-coupled receptor binding	6	224	13	7079	3.11E-05	8.18E-02
Chemokine receptor binding	6	224	13	7079	3.11E-05	8.18E-02
Caspase activity	5	224	10	7079	0.000173376	4.57E-01

[a] HUVEC were incubated alone and in the presence of IFN-α (1000 IU/ml) for 5 h and RNA was expression analyzed by microarrays as detailed in *Materials and Methods*. EASE, Expression Analysis Systematic Explorer.

Table III. *Top 50 IFN-α-induced genes in HUVEC[a]*

Probe Set	Gene Symbol	Description	Fold Induction
213797_at	CIG5	Viperin	1361.98
203153_at	IFIT1	IFN-induced protein with tetratricopeptide repeats 1	721.68
211122_s_at	CXCL11	Chemokine (C-X-C motif) ligand 11	459.25
210163_at	CXCL11	Chemokine (C-X-C motif) ligand 11	373.84
204533_at	CXCL10	Chemokine (C-X-C motif) ligand 10	354.70
204439_at	C1orf29	Chromosome 1 open reading frame 29	298.73
204994_at	MX2	Myxovirus (influenza virus) resistance 2 (mouse)	268.70
205660_at	OASL	2′,5′-Oligoadenylate synthetase-like	203.92
202086_at	MX1	Myxovirus (influenza virus) resistance 1	198.44
204747_at	IFIT4	IFN-induced protein with tetratricopeptide repeats 4	192.79
210797_s_at	OASL	2′,5′-Oligoadenylate synthetase-like	179.89
217502_at	IFIT2	IFN-induced protein with tetratricopeptide repeats 2	172.63
204972_at	OAS2	2′,5′-Oligoadenylate synthetase 2 (69/71 kDa)	167.78
205552_s_at	OAS1	2′,5′-Oligoadenylate synthetase 1 (40/46 kDa)	125.62
202869_at	OAS1	2′,5′-Oligoadenylate synthetase 1 (40/46 kDa)	120.57
219863_at	CEB1	Cyclin E-binding protein 1	88.03
219684_at	IFRG28	IFN-responsive protein (28 kDa)	86.55
210029_at	INDO	Indoleamine-pyrrole 2,3-dioxygenase	82.27
204279_at	PSMB9	Proteasome (prosome, macropain) subunit, β-type, 9	63.30
219352_at	FLJ20637	Hypothetical protein FLJ20637	63.22
204415_at	G1P3	IFN, α-inducible protein (clone IFI-6-16)	62.83
218943_s_at	DDX58	DEAD/H (Asp-Glu-Ala-Asp/His) box polypeptide	50.65
214453_s_at	IFI44	IFN-induced protein 44	46.55
219209_at	MDA5	Melanoma differentiation associated protein-5	44.36
213716_s_at	SECTM1	Secreted and transmembrane 1	39.84
206271_at	TLR3	Toll-like receptor 3	39.37
214059_at	IFI44	IFN-induced protein 44	35.83
202269_x_at	GBP1	Guanylate binding protein 1, IFN-inducible (67 kDa)	33.09
208436_s_at	IRF7	IFN regulatory factor 7	32.03
219593_at	SLC15A3	Peptide transporter 3	31.79
218400_at	OAS3	2′,5′-Oligoadenylate synthetase 3 (100 kDa)	31.74
209417_s_at	IFI35	IFN-induced protein 35	31.58
214022_s_at	IFITM1	6-Pyruvoyltetrahydropterin synthase	30.14
203148_s_at	TRIM14	Tripartite motif-containing 14	29.98
219691_at	FLJ20073	Hypothetical protein FLJ20073	27.03
202270_at	GBP1	Guanylate binding protein 1, IFN-inducible (67 kDa)	25.60
201601_x_at	IFITM1	6-Pyruvoyltetrahydropterin synthase	25.16
221766_s_at	C6orf37	Chromosome 6 open reading frame 37	24.29
204224_s_at	GCH1	GTP cyclohydrolase 1 (dopa-responsive dystonia)	23.95
205483_s_at	G1P2	INF, α-inducible protein (clone IFI-15K)	22.86
209762_x_at	SP110	SP110 nuclear body protein	22.85
203595_s_at	IFIT5	Retinoic acid- and IFN-inducible protein (58 kDa)	22.48
209761_s_at	SP110	SP110 nuclear body protein	22.14
219716_at	APOL6	Apolipoprotein L, 6	21.88
202687_s_at	TNFSF10	TNF superfamily, member 10 (TRAIL)	21.11
208012_x_at	SP110	SP110 nuclear body protein	20.91
210785_s_at	C1orf38	Basement membrane-induced gene	20.58
203596_s_at	IFIT5	Retinoic acid- and IFN-inducible protein (58 kDa)	19.62
208392_x_at	SP110	SP110 nuclear body protein	19.39
205170_at	STAT2	Signal transducer and activator of transcription 2 (113 kDa)	17.27

[a] HUVEC were incubated alone and in the presence of IFN-α (1000 IU/ml) for 5 h and RNA expression was analyzed by microarrays as detailed in *Materials and Methods*.

The q values were between 0.012 and 0.0031 for the different gene lists created. Annotations were obtained through the Database for Annotation, Visualization, and Integrated Discovery (DAVID; http://david.niaid. nih.gov/david/beta/index.htm) (23). The microarray data discussed in this publication have been deposited in the Gene Expression Omnibus (GEO; www.ncbi.nlm.nih.gov/geo/info/linking.html) of the National Center for Biotechnology Information and are accessible through GEO series accession number GSE3920.

RT-PCR end-point analysis

The expressions of murine *CXCL10*, *CXCL11*, *TRAIL*, and *β-actin* were analyzed by qualitative PCR. Briefly, total RNA was extracted from in vitro cultured cells and homogenized tumors as described above, and RNA was reverse transcribed using 12.5 U of avian myeloblastosis virus reverse transcriptase and 0.5 µg of (oligo)dT as primer for 45 min at 42°C and 5 min at 99°C. The following set of primers (Sigma-Genosys) was used: CXCL10 forward, 5′-ACCATGAACCCAAGTGCTGCCGTC-3′; CXCL10 reverse, 5′-GCTTCACTCCAGTTAAGGAGCCCT-3′; CXCL11

forward, 5′-AGGAAGGTCACACCATAGC-3′; CXCL11 reverse, 5′-CAG GTTCCTGGCACAGAGTT-3′; TRAIL forward, 5′-TCACCAACGAGAT GAAGCAG-3′; TRAIL reverse, 5′-GCCTAAGGTCTTTCCATCC-3′; murine β-actin forward, 5′-CCTTCCTGGGCATGGAGTCCTG-3′; and murine β-actin reverse 5′-GGAGCAATGATCTTGATCTTC-3′.

In each amplification, cDNA from a cell line known to express a given factor was included as the positive control. Water was used as a negative control. PCR was performed for 30 cycles at 95°C for 1 min, 58°C for 1 min, and 72°C for 1 min in a total volume of 50 µl using GoldTaq and standard PCR buffers (all from Applied Biosystems). The amplified products were resolved by 1.5% agarose gel electrophoresis and stained with ethidium bromide. No bands were obtained by PCR analysis of RNA samples amplified without RT.

Quantitative RT-PCR

Expression data validation was performed by quantitative real-time RT-PCR using the RNA extracted from IFN- or mock-treated cells and reverse transcribed as described above with oligo(dT) primers in a 20-µl final

Table IV. *Differentially responsive genes in IFN-α- and IFN-γ-treated HUVEC[a]*

Probe Set	Gene Symbol	Description	IFN-α	IFN-γ	αγ
213797_at	cig5	Viperin	1362.0[b]	3.0[b]	448.1
204994_at	MX2	Myxovirus (influenza virus) resistance 2 (mouse)	268.7	1.2	232.0
203153_at	IFIT1	IFN-induced protein with tetratricopeptide repeats 1	721.7	4.1	174.2
210797_s_at	OASL	2′,5′-Oligoadenylate synthetase-like	179.9	1.2	146.2
205660_at	OASL	2′,5′-Oligoadenylate synthetase-like	203.9	1.8	112.9
219863_at	CEB1	Cyclin E-binding protein 1	88.0	0.9	94.6
204415_at	G1P3	IFN, α-inducible protein (clone IFI-6-16)	62.8	2.4	25.7
217502_at	IFIT2	IFN-induced protein with tetratricopeptide repeats 2	172.6	6.8	25.5
219352_at	FLJ20637	Hypothetical protein FLJ20637	63.2	3.5	18.3
202086_at	MX1	Myxovirus (influenza virus) resistance 1	198.4	12.3	16.1
202869_at	OAS1	2′,5′-Oligoadenylate synthetase 1 (40/46 kDa)	120.6	8.0	15.1
221766_s_at	C6orf37	Chromosome 6 open reading frame 37	24.3	1.8	13.6
205552_s_at	OAS1	2′,5′-Oligoadenylate synthetase 1 (40/46 kDa)	125.6	10.4	12.1
204972_at	OAS2	2′,5′-oligoadenylate synthetase 2 (69/71 kDa)	167.8	14.1	11.9
207571_x_at	C1orf38	Basement membrane-induced gene	14.8	1.3	11.1
204439_at	C1orf29	Chromosome 1 open reading frame 29	298.7	27.5	10.9
218943_s_at	DDX58	DEAD/H (Asp-Glu-Ala-Asp/His) box polypeptide	50.6	4.9	10.4
200606_at	DSP	Desmoplakin (DPI, DPII)	11.1	1.1	10.1
210785_at	C1orf38	Basement membrane-induced gene	20.6	2.1	9.7
208436_s_at	IRF7	IFN regulatory factor 7	32.0	3.5	9.2
219691_at	FLJ20073	Hypothetical protein FLJ20073	27.0	2.9	9.2
205483_s_at	G1P2	IFN, α-inducible protein (clone IFI-15K)	22.9	2.6	8.9
203148_s_at	TRIM14	Tripartite motif-containing 14	30.0	3.6	8.3
219684_at	IFRG28	IFN-responsive protein (28 kDa)	86.6	10.5	8.2
204698_at	ISG20	IFN-stimulated gene (20 kDa)	15.7	2.0	7.8
214059_at	IFI44	IFN-induced protein 44	35.8	4.7	7.7
214453_s_at	IFI44	IFN-induced protein 44	46.5	6.1	7.6
218400_at	OAS3	2′,5′-Oligoadenylate synthetase 3 (100 kDa)	31.7	4.2	7.6
209493_at	PDZK3	PDZ domain-containing 2	5.8	0.8	7.5
33304_at	ISG20	IFN-stimulated gene (20 kDa)	14.3	2.0	7.1
221371_at	TNFSF18	TNF (ligand) superfamily, member 18	5.5	0.8	7.0
219209_at	MDA5	Melanoma differentiation associated protein-5	44.4	6.4	6.9
219364_at	LGP2	Likely ortholog of mouse D11lgp2	8.6	1.3	6.6
219011_at	PLEKHA4	Pleckstrin homology domain containing, family A member 4	7.2	1.1	6.6
206271_at	TLR3	Toll-like receptor 3	39.4	6.0	6.5
204187_at	GMPR	Guanosine monophosphate reductase	6.4	1.0	6.3
219211_at	USP18	Ubiquitin specific protease 18	17.1	3.1	5.5
202357_s_at	BF	B-factor, properdin	6.9	1.3	5.3
206553_at	OAS2	2′,5′-Oligoadenylate synthetase (269/71 kDa)	13.9	2.6	5.3
204747_at	IFIT4	IFN-induced protein with tetratricopeptide repeats 4	192.8	37.7	5.1
213361_at	TDRD7	Tudor repeat associator with PCTAIRE 2	9.5	1.9	5.0
203140_at	BCL6	B-cell CLL/lymphoma 6 (zinc finger protein 51)	0.9	4.2	0.2
210029_at	INDO	Indoleamine-pyrrole 2,3 dioxygenase	82.3	407.9	0.2
204070_at	RARRES3	Retinoic acid receptor responder (tazarotene induced) 3	7.0	37.9	0.2
216048_s_at	RHOBTB3	Rho-related BTB domain-containing 3	0.8	4.9	0.2
205890_s_at	UBD	Ubiquitin D	3.0	61.1	0.0
204057_at	ICSBP1	IFN consensus sequence-binding protein 1	1.1	26.4	0.0

[a] HUVEC were incubated alone and in the presence of IFN-α or IFN-γ for 5 h and RNA expression was analyzed as detailed in *Materials and Methods*. The genes showing a >5-fold difference between IFN-α-treated and IFN-γ-treated samples are listed.
[b] Fold induction as compared to control HUVEC.

volume. All primers for the genes tested were designed using Primer3 software (24) with a T_m optimum of ~60°C and a product length of 100–150 nt (Table I). Real-time PCR was performed on an I-Cycler (Bio-Rad) using iQ Supermix (Bio-Rad) supplemented with 10 nM fluorescein (Bio-Rad), 0.1× SYBR Green I (Sigma-Aldrich), 2.5 μl of cDNA (5× diluted), and 0.3 μM sense and antisense primers in a final reaction volume of 25 μl. After an initial denaturation step of 3 min during which the well factor was measured, 50 cycles of 15 s at 95°C followed by 30 s at 60°C were performed. Fluorescence was measured during the annealing step in each cycle. After amplification, melt curves with 80 steps of 15 s and 0.5°C increase were performed to monitor amplicon identity. Amplification efficiency was assessed for all primer sets used in separate reactions, and primers with efficiencies >94% were used. Expression data were normalized on GAPDH and RNA polymerase II gene expression data obtained in parallel. Relative expression values with SE values and statistical comparisons (unpaired two-tailed *t* test) were obtained using QGene software (25). Expression changes were calculated from the mean value of normalizations obtained using the above genes as references.

Quantification of CXCL10, CXCL11, and TRAIL protein levels

ELISA (R&D Systems) were used to quantify the levels of CXCL10 and CXCL11 in the supernatants of EC and HF incubated for 48 h in the presence of IFN-α or IFN-γ as described above. In the kinetics experiments, HUVEC were treated with either IFN-α or IFN-γ for 5 h and washed and cultivated for various intervals (range, 18–72 h) in complete medium without IFNs. The range of sensitivity of the assays was 7.8–500 pg/ml and 62.5–4000 pg/ml for CXCL10 and CXCL11, respectively. Concentrations of TRAIL in cell-free supernatants and cell lysates were measured by ELISA (Diaclone Research), according to manufacturer's instructions.

In vivo tumor growth

Parental or IFN-α-producing MCF7 cells were injected s.c. into the flanks of female SCID mice (5 × 10⁵ cells/mouse) obtained from Charles River Breeding Laboratories. Tumor size was measured daily with calipers; when

FIGURE 1. Real-time PCR validation of microarray data. *A*, Real-time PCR analysis was performed as described in *Materials and Methods* using primers listed in Table I and cDNA prepared from IFN-α- or IFN-γ-treated HUVEC. Results indicate the log of relative expression of the individual genes listed on the *y*-axis, as judged by microarray analysis (MA; gray columns) and real-time PCR (RT; filled columns). Real-time PCR data were normalized on GAPDH and RNA polymerase II expression levels; the mean value is reported as log 2. *B*, Real-time PCR analysis of *CXCL10* and *CXCL11* expression in HUVEC and HF incubated in the absence (gray columns) and the presence of IFN-α (open columns) or IFN-γ (filled columns).
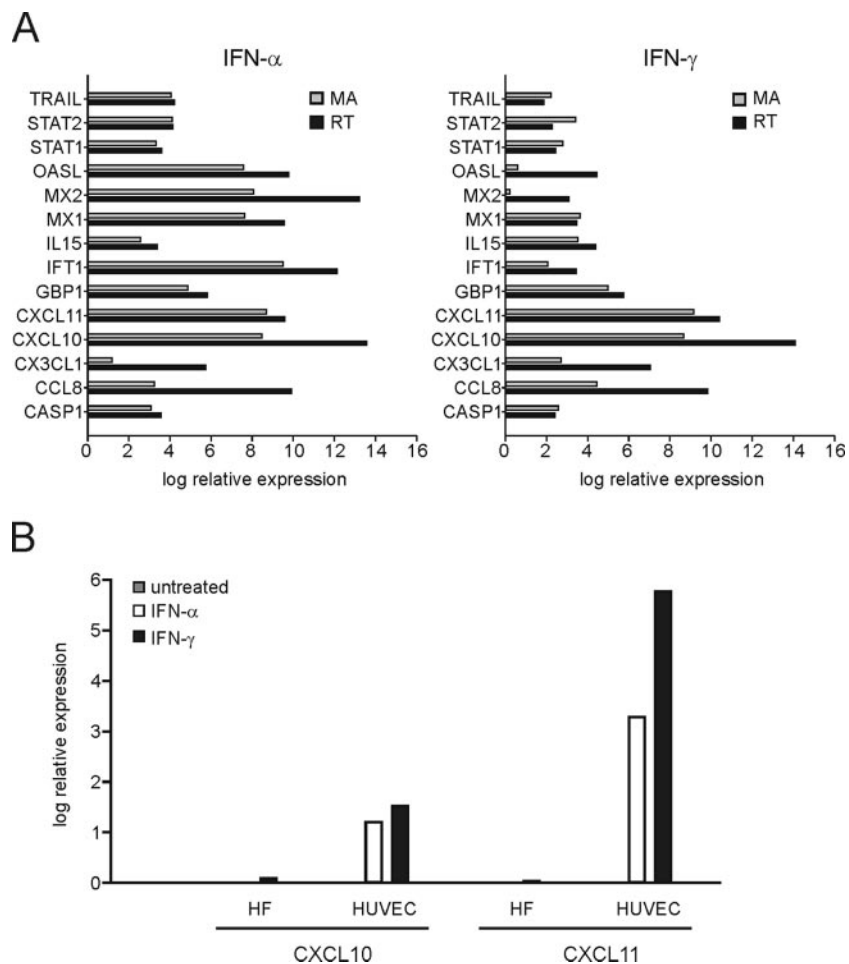
8control tumors were ~300 mm³, the animals were sacrificed and the tumors collected. The tumors were either snap frozen or fixed in formalin, paraffin-embedded, sectioned, and stained with H&E for histological analysis. Procedures involving animals and their care conformed with institutional guidelines that comply with national and international laws and policies (European Economic Community Council Directive 86/609, OJ L 358, 1, Dec. 12, 1987; National Institutes of Health Guide for the Care and Use of Laboratory Animals, National Institutes of Health Publication 85-23, 1985).

Histology and immunohistochemistry

Four-micrometer thick sections of MCF7 tumors were rehydrated and either stained with H&E or processed for immunohistochemistry by standard procedures. The sections were labeled with a goat anti-CXCL11 Ab (Santa Cruz Biotechnology), and immunostaining was performed using the avidin-biotin-peroxidase complex technique and 3,3′-diaminobenzidine as a chromogen (Vector Laboratories). Sections were finally lightly counterstained with Mayer's hematoxylin. Parallel negative controls obtained by replacing primary Abs with PBS were run in all cases.

Western blot analysis of guanylate-binding protein (GBP)-1 expression

GBP-1 expression in tumor and cell lysates was determined by Western blotting according to standard protocols. Briefly, tumor samples were run on 10% polyacrylamide gels; separated proteins were then blotted for 2 h at 400 mA onto a nitrocellulose membrane. The membrane was then saturated with PBS plus 1% nonfat dry milk (Sigma-Aldrich) as blocking buffer for 3 h at room temperature and then stored at −20°C until use. Immunoprobing was performed with rabbit polyclonal Abs against human GBP-1 used at 0.1 μg/ml (Santa Cruz Biotechnology), followed by hybridization with a 1/5000 diluted anti-rabbit HRP-conjugated Ab (Amersham Biosciences). Ags were identified by luminescent visualization using

the SuperSignal kit (Pierce). Tubulin was used to normalize differences among the different lanes.

Migration assay

To test the inhibitory activity of IFNs, HMVEC were cultured for 48 h with complete EBM-2 medium supplemented with either IFN-α or IFN-γ (1000 U/ml) before the migration assay. In some wells, CXCL10 (50 nM; Peprotech) was added to the HMVEC as a positive control. To inhibit CXCR-3-mediated effects on EC migration, a neutralizing anti-human CXCR3 mAb was used (IgG1, clone 49801.111, final concentration 10 μg/ml; R&D Systems). Isotype-matched (IgG1) controls were also included in each experiment to check for the specificity of the effects of the anti-CXCR3 mAb.

Chemotaxis assays were performed in Boyden chambers using poly-vinylpyrrolidone-free polycarbonate filters with 12-μm pores for HMVEC cells coated with 5 μg of collagen IV. HMVEC (1.2×10^5) pretreated with IFNs, CXCL10, or appropriate Abs were placed in the upper compartment in a serum-free medium containing 0.1% BSA; the lower compartment of the chamber was filled with either conditioned medium from the Kaposi's sarcoma-derived KS-IMM cell line (26) as a chemoattractant or SFM as a negative control. The chambers were then incubated at 37°C in 5% CO_2 for 3 h. Cells remaining on the upper surface of the filter were then mechanically removed, and 5–10 random fields of cells that had migrated to the lower surface of each filter were stained and counted. Assays were performed in triplicate and repeated at least three times.

Angiogenesis assay

The Matrigel sponge model of angiogenesis was used as previously described (26). Angiogenic growth factors, including vascular endothelial growth factor (100 ng/ml), TNF-α (2 ng/ml), and heparin (24–26 U/ml) (VTH; all from PeproTech), were added to liquid Matrigel at 4°C. In some experiments, IFN-γ (1000 U/ml), anti-mouse-CXCR3 (15

Table V. *Differentially responsive genes in IFN-α-treated HUVEC and HF[a]*

Probe Set	Gene Symbol	Description	HUVEC	HF	Ratio
210163_at	CXCL11	Chemokine (C-X-C motif) ligand 11	373.8[b]	0.6[b]	645.0
211122_s_at	CXCL11	Chemokine (C-X-C motif) ligand 11	459.3	1.1	418.8
210029_at	INDO	Indoleamine-pyrrole 2,3-dioxygenase	82.3	2.8	29.8
219863_at	CEB1	Cyclin E-binding protein 1	88.0	3.1	28.6
204533_at	CXCL10	Chemokine (C-X-C motif) ligand 10	354.7	20.2	17.6
219691_at	FLJ20073	Hypothetical protein FLJ20073	27.0	1.7	15.6
214329_x_at	TNFSF10	TNF (ligand) superfamily, member 10	13.5	0.9	14.7
204070_at	RARRES3	Retinoic acid receptor responder (tazarotene induced) 3	7.0	0.5	12.9
219209_at	MDA5	Melanoma differentiation associated protein-5	44.4	3.5	12.6
214059_at	IFI44	IFN-induced protein 44	35.8	3.1	11.6
213797_at	cig5	Vipirin	1362.0	121.0	11.3
220351_at	CCRL1	Chemokine (C-C motif) receptor-like 1	5.0	0.5	11.0
219684_at	IFRG28	IFN responsive protein (28 kDa)	86.6	8.9	9.7
209546_s_at	APOL1	Apolipoprotein L, 1	12.4	1.3	9.4
202748_at	GBP2	Guanylate-binding protein 2, IFN-inducible	5.1	0.6	8.9
202687_s_at	TNFSF10	TNF (ligand) superfamily, member 10	21.1	2.5	8.5
221371_at	TNFSF18	TNF (ligand) superfamily, member 18	5.5	0.6	8.5
205552_s_at	OAS1	2′,5′-Oligoadenylate synthetase 1 (40/46 kDa)	125.6	15.2	8.3
221766_s_at	C6orf37	Chromosome 6 open reading frame 37	24.3	2.9	8.2
205890_s_at	UBD	Ubiquitin D	3.0	0.4	7.4
202688_at	TNFSF10	TNF (ligand) superfamily, member 10	15.5	2.2	7.1
202270_at	GBP1	Guanylate-binding protein 1, IFN-inducible (67 kDa)	25.6	3.7	6.8
206271_at	TLR3	Toll-like receptor 3	39.4	5.9	6.6
206693_at	IL7	Interleukin 7	3.8	0.6	6.6
209493_at	PDZK3	PDZ domain-containing 2	5.8	0.9	6.4
203153_at	IFIT1	IFN-induced protein with tetratricopeptide repeats 1	721.7	115.3	6.3
206011_at	CASP1	Caspase 1, apoptosis-related cysteine protease	7.7	1.3	6.2
38241_at	BTN3A3	Butyrophilin, subfamily 3, member A3	4.2	0.7	6.1
205467_at	CASP10	Caspase 10, apoptosis-related cysteine protease	3.3	0.5	6.0
221245_s_at	DKFZP434E2135	Hypothetical protein DKFZp434E2135	3.3	0.5	6.0
212081_x_at	BAT2	HLA-B associated transcript 2	1.0	0.2	5.8
213716_s_at	SECTM1	Secreted and transmembrane 1	39.8	7.0	5.7
210538_s_at	BIRC3	Baculoviral IAP repeat-containing 3	2.2	0.4	5.6
221087_s_at	APOL3	Apolipoprotein L, 3	7.4	1.3	5.6
204205_at	APOBEC3G	Apolipoprotein B mRNA editing enzyme	8.1	1.5	5.4
210797_s_at	OASL	2′,5′-Oligoadenylate synthetase-like	179.9	33.5	5.4
200606_at	DSP	Desmoplakin (DPI, DPII)	11.1	2.1	5.4
203595_s_at	IFIT5	Retinoic acid- and IFN-inducible protein (58 kDa)	22.5	4.2	5.4
217371_s_at	IL15	Interleukin 15	4.4	0.8	5.3
219364_at	LGP2	Likely ortholog of mouse D11lgp2	8.6	1.6	5.3
58916_at	KCTD14	Hypothetical protein MGC2376	5.9	1.1	5.2
214022_s_at	IFITM1	6-Pyruvoyltetrahydropterin synthase	30.1	150.8	0.2
206911_at	TRIM25	Zinc finger protein	3.5	18.8	0.2
203610_s_at	TRIM38	Tripartite motif-containing 38	4.0	21.4	0.2
209040_s_at	PSMB8	Proteasome (prosome, macropain) subunit, β-type, 8	6.8	45.6	0.1
218543_s_at	ZC3HDC1	Hypothetical protein FLJ22693	6.0	41.7	0.1
201641_at	BST2	Bone marrow stromal cell antigen 2	10.9	91.9	0.1
202411_at	IFI27	IFN, α-inducible protein 27	4.3	71.6	0.1

[a] HUVEC or HF were incubated alone and in the presence of IFN-α for 5 h and RNA expression was analyzed as detailed in *Materials and Methods*. The genes showing a >5-fold difference between IFN-α-treated HUVEC and HF are listed.
[b] Fold induction as compared to control cells.

μg/ml), or control isotype Ab (15 μg/ml) (R&D Systems) were added to the Matrigel. This suspension (final volume of 600 μl) was slowly injected s.c. into the flanks of 6-wk-old male C57BL/6 mice, where the Matrigel polymerizes to form a solid gel. After 4 days, gels were recovered, weighed, minced, and diluted in water and the hemoglobin content was measured with a Drabkin reagent kit (Sigma-Aldrich). The final hemoglobin concentration was calculated from a standard calibration curve.

Results

Genes induced by IFNs in HUVEC

Analysis of the gene expression profile in HUVEC after 5 h of activation by IFN-α indicated that numerous genes were induced and only a few were down-regulated; 356 probe sets were >2-fold up-regulated and 23 probe sets were >2-fold down-regulated. Two hundred forty-two of the up-regulated and none of the down-regulated probe sets were found to be statistically significant after testing using Significance Analysis of Microarrays (delta value set

to return a median false significant number <1, q = 0.003; see also supplemental Table I).[5] Of these probe sets, 137 corresponded to unique, characterized genes, 67 of which were present with two or more probe sets, and 38 corresponded to unknown genes.

We next analyzed gene ontology classes of the genes induced. The ratio of IFN-α-induced genes belonging to a given gene ontology class (list hits) and the total of annotated genes present in this list (list total) were compared with the ratio of expressed, annotated genes belonging to the same ontology (population hits) and the total of expressed, annotated genes present on the array (population total). Statistical significance was analyzed using the Expression Analysis Systematic Explorer (EASE) score as well as Bonferroni multiparameter posttesting. The most significant gene

---

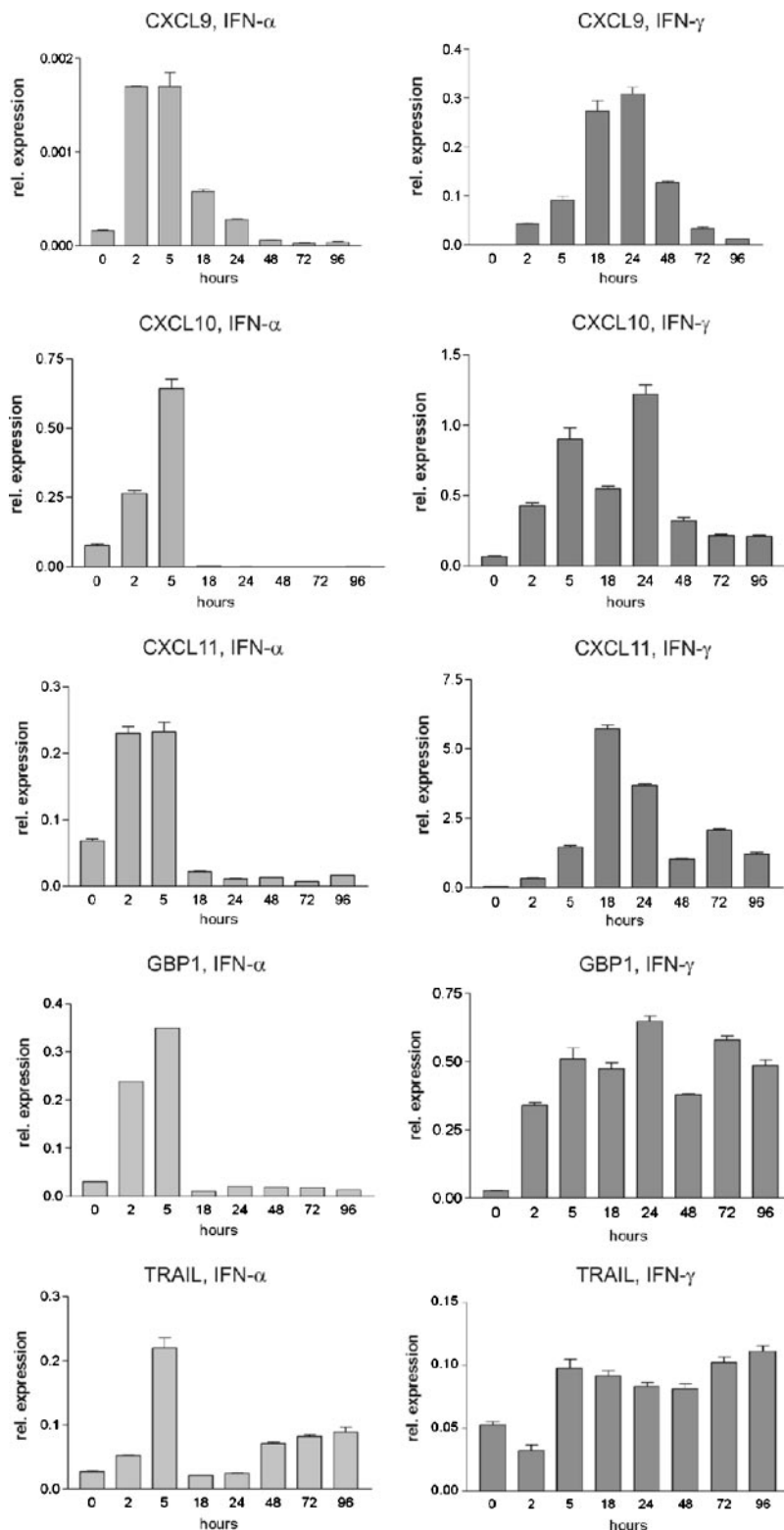[5] The online version of this article contains supplemental material.

FIGURE 2. Time course analysis of gene expression in IFN-activated HUVEC. Real-time PCR analysis of CXCL9–11, GBP-1, and TRAIL expression was performed as described in *Materials and Methods* using primers listed in Table I and cDNA prepared from IFN-α- or IFN-γ-treated HUVEC. RNA was extracted from HUVEC at the time points indicated in the *x*-axis. Treatment with IFNs (1000 U/ml) lasted up to 5 h and was then followed by washing, replacement with fresh culture medium without IFN, and cultivation for the indicated times before RNA extraction (range, 18–96 h). Results indicate the log of relative (rel.) expression of the individual genes on the *y*-axis as judged by real-time PCR. Data were normalized on GAPDH and RNA polymerase II expression levels; the mean value is reported as log 2.

ontology classes corresponded to the biological processes of defense/immune/inflammatory responses and molecular functions compatible with their involvement in these processes, including cytokine and chemokine activity (Table II). This is in general agreement with other reports on the classes of IFN-α-stimulated genes (12, 15, 16, 18).

Viperin, an IFN-inducible antiviral protein that is also directly induced by the CMV (27), and *IFIT1*, a member of the IFN-regulated *IFI54/IFI56* family (28), were the highest responding genes

in HUVEC, being induced 1362-fold and 722-fold, respectively, following IFN-α treatment (Table III). Interestingly, transcription of two members of the ELR$^-$ CXC chemokine family (29), *CXCL10* and *CXCL11*, was also strongly induced by IFN-α in these cells; the relative probe sets showed 459/374-fold induction for *CXCL11* and 355-fold induction for *CXCL10* as compared with untreated controls. Table III reports the 50 most strongly IFN-α-induced genes in HUVEC (for a complete list of induced genes see supplemental Table I[5]).
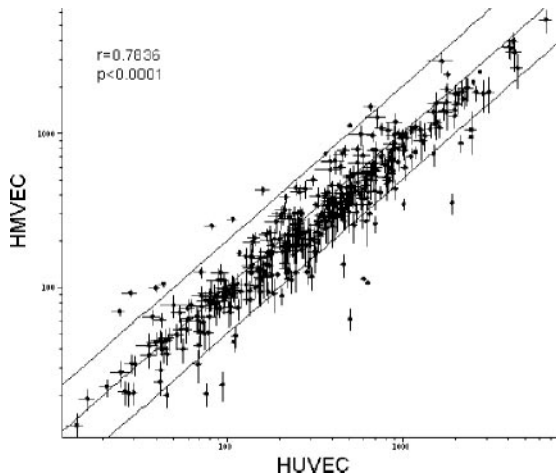
FIGURE 3. Scatter plot of expression values of genes induced by IFN-α or IFN-γ in HUVEC and HMVEC. Very few genes show differential expression exceeding the 2-fold interval delimited by the diagonals. Bars indicate SEM; r and p values were obtained by Pearson's correlation.

IFN-β treatment induced changes in the transcriptome of HUVEC that were virtually identical with those obtained following IFN-α stimulation (data not shown); for this reason, no replicates and statistical evaluations for IFN-β were performed. In contrast, several genes were differentially up-regulated by class I and class II IFN in HUVEC. Forty-seven genes showed a >5-fold difference upon induction with the two types of IFN and 14 of them were induced >5-fold by IFN-α and <2-fold by IFN-γ (Table IV). Both *CXCL10* and *CXCL11* were strongly up-regulated by IFN-γ also (591/550-fold and 408-fold, respectively). A few genes were up-regulated by IFN-γ but showed little response to class I IFNs; among these, we found *CXCL9*, which was increased by 228-fold following IFN-γ treatment. Due to high variability between independent experiments (69- to 387-fold induction), *CXCL9* was not among the genes that passed statistical testing; notwithstanding, its preferential up-regulation by IFN-γ was confirmed by real-time PCR analysis for other EC types (see below).

Validation of expression data by real-time PCR

We then validated the microarray gene expression data by means of real-time PCR for a group of genes (Fig. 1A). In addition to the most strongly up-regulated genes, including *CXCL10* and *CXCL11*, we selected several other genes that were induced to a lesser extent (comprised in supplementary Table I), including some genes potentially involved in angiogenesis control such as *TRAIL* (also called *TNFSF10*) and *GBP-1*. Although some variation in the extent of regulation was observed, the data obtained with microarrays were substantially confirmed by real-time PCR analysis (Fig. 1A). Only in the case of *OASL* and *MX2* did we observe a dramatic discrepancy between microarray and real-time PCR data for IFN-γ-treated HUVEC (Fig. 1A); however, if the ratio between the signals in IFN-α-treated and IFN-γ-treated cells was considered, the differential responsiveness was still confirmed (*MX2*: microarray IFN-α vs IFN-γ = 232-fold, RT-PCR 1115-fold; *OASL*: microarray IFN-α vs γ = 146/113-fold, RT-PCR 102-fold). All expression variations were statistically significant (unpaired *t* test, $p < 0.05$). Major quantitative differences between microarray and RT-PCR analyses occurred for genes that were not expressed in untreated HUVEC, because background adjustment by GeneChip robust multi-array average leaves unexpressed genes at an intensity above zero.

EC-specific transcriptional changes induced by IFN-α

To explore to what extent the transcriptional changes detected in HUVEC following IFN treatment were lineage-specific, we compared the effect of IFN-α on the microarray expression profile of HUVEC and primary HF. Of note, HUVEC and HF were both derived from single umbilical cord samples and were thus representative of two different normal cell types from a same donor. IFN-α treatment produced marked transcriptional changes also in HF, with >2-fold statistically significant ($q = 0.012$) changes in the expression levels of 235 genes. The great majority (80%) of genes induced by IFN-α were the same in both cell types (<5-fold difference); however, some quantitative and/or qualitative differences were observed. A list of the genes differentially expressed in HUVEC and HF upon IFN-α treatment is shown in Table V; in particular, *CXCL11* was apparently not induced in HF by IFN-α,

Table VI. *IFN-dependent gene regulation in different endothelial cell types*[a]

Gene Identifier	HUVEC IFN-α	HUVEC IFN-γ	HMVEC 1 IFN-α	HMVEC 1 IFN-γ	HMVEC 2 IFN-α	HMVEC 2 IFN-γ	HMVAR IFN-α	HMVAR IFN-γ
CASP1	12	5	9	5	8	6	13	7
CCL8	958	921	33	97	66	776	128	1528
CX3CL1	53	131	5	15	72	736	84	521
CXCL10	12107	17334	1930	4204	13751	48822	2986	8711
CXCL11	771	1350	407	1405	*1357*	*7774*	84	325
CXCL9	649	809	702	50058	158	75418	2257	163113
GBP1	56	53	58	116	*1*	*0*	21	36
IFIT1	4454	11	1102	4	*2358*	*31*	1429	19
IL15	10	21	9	25	*13*	*44*	21	56
MX1	752	11	188	11	486	79	120	17
MX2	9536	9	258	2	*1690*	*51*	584	18
OASL	876	22	232	3	*358*	*20*	683	33
P53	1	1	1	1	*1*	*1*	1	1
STAT1	12	5	7	5	12	6	11	8
STAT2	18	5	14	2	12	9	13	9
TNSF10	18	4	16	4	*8*	*4*	245	43

[a] cDNAs obtained from different EC types were analyzed by real-time PCR for the expression of 16 genes and normalized to RNA polymerase II and GAPDH expression. Expression values are indicated as fold change over untreated controls. Numbers in italics correspond to data normalized on RNA polymerase II, but overlapping results were obtained by normalization against GAPDH.
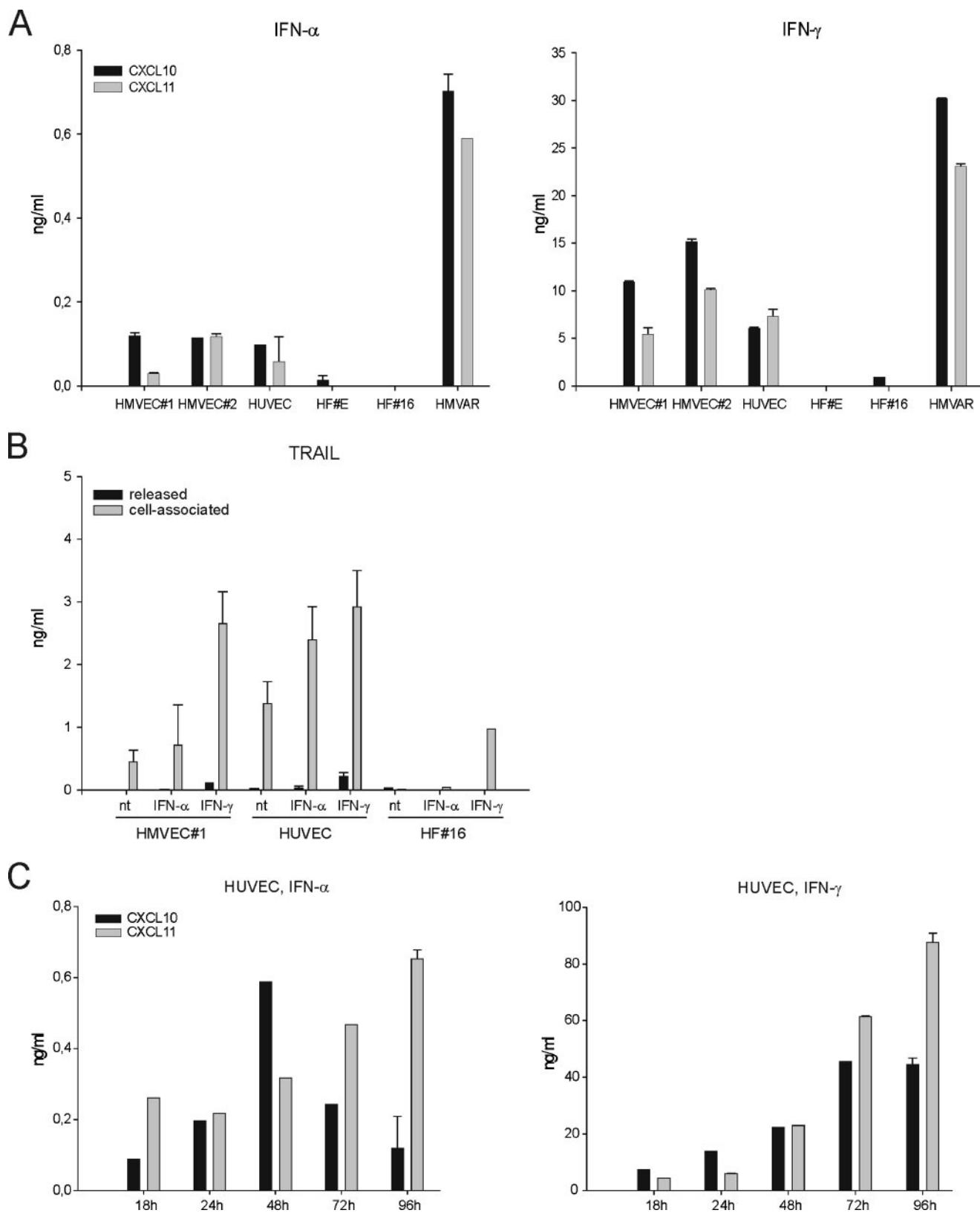
FIGURE 4. Production of CXCL10, CXCL11, and TRAIL in the supernatants of IFN-stimulated cells. *A,* Different types of EC including microvascular EC (HMVEC 1 (HVEC#1) and HMVEC 2 (HMVEC#2)), HUVEC, and HMVAR, as well as human primary fibroblasts (HF E (HF#E) and HF 16 (HF#16)) were cultured for 48 h alone and in the presence of IFN-α or IFN-γ (1000 IU/ml). The amount of CXCL10, CXCL11, and TRAIL in the supernatants or cell lysates was measured in triplicate by ELISA. CXCL10 and CXCL11 levels in the supernatants of untreated cells were always below the sensitivity limits of the assay. Three independent experiments were performed; the error bars indicate the SD from the mean. nt, Untreated samples. Kinetics of CXCL10 and CXCL11 production by HUVEC. EC were cultured for 5 h in the presence of IFN-α or IFN-γ (1000 IU/ml); after washing, fresh medium without IFNs was added and the supernatants were collected at the indicated time points thereafter. Supernatants from four different HUVEC cultures were pooled and analyzed by ELISA to measure the amounts of CXCL10 and CXCL11. Three independent experiments were performed; the error bars indicate the SD from the mean.
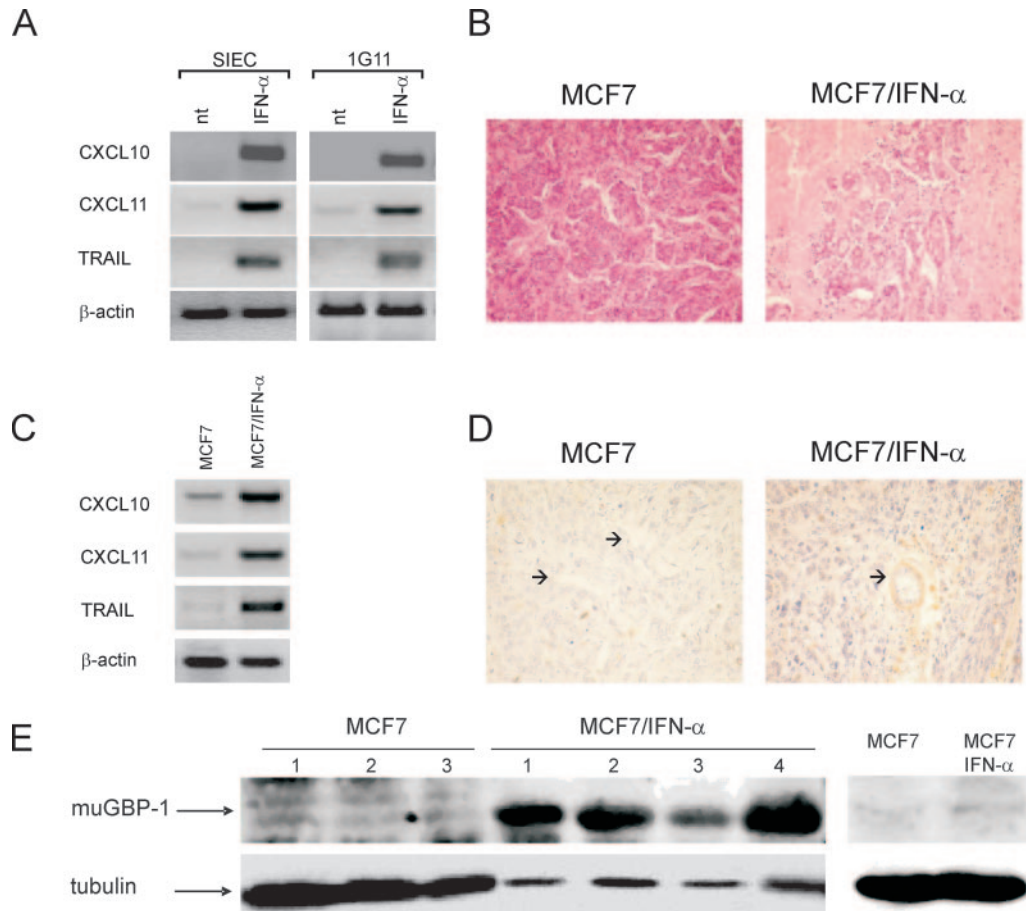
FIGURE 5. In vitro and in vivo effects of IFN-α on the expression of CXCL10, CXCL11, and TRAIL by murine EC. *A*, SIEC (lung microvascular cell line) and 1G11 (dermal microvascular cell line) were incubated alone (nt) and in the presence of IFN-α; the expression of the genes listed on the *left* was analyzed by RT-PCR. *B*, Groups of SCID mice were injected s.c. with cells of the MCF7 tumor cell line, either untreated or engineered to express murine IFN-α (MCF7/IFN-α). H&E staining of tumor masses shows large areas of necrosis in IFN-α-expressing tumors. *C*, The RNA obtained from IFN-α-producing or control MCF7 tumor samples was analyzed by RT-PCR for expression of murine CXCL10, *CXCL11*, and *TRAIL*. β-Actin was used as an amplification control. *D*, Immunohisto-chemical analysis of CXCL11 expression in IFN-α-expressing tumors. Staining with anti-CXCL11 Ab disclosed CXCL11 expression in some blood vessels (arrow) within IFN-α-producing but not control tumors (original magnification, ×400). *E*, Western blot analysis of GBP-1 expression in IFN-α-expressing tumors. Hybridization with anti-GBP-1 Ab showed increased murine GBP-1 (muGBP-1) expression in IFN-α-expressing tumors (MCF7/IFN-α) than in controls (MCF7). Tubulin hybridization is shown as a loading control. Expression of GBP-1 in cell lysates from MCF7 cells treated in vitro with IFN-α or control cells is shown in the *right panel*.

whereas *CXCL10*, although induced, showed a 18 times lower in-duction than in HUVEC. Real-time PCR analysis confirmed the EC-specific up-regulation of *CXCL10* and *CXCL11* following both IFN-α and IFN-γ treatment (Fig. 1*B*).

Kinetics of gene expression in IFN-stimulated EC

To investigate the dynamics of the transcriptional changes induced by IFNs in EC, a time course analysis was performed. HUVEC were stimulated with 1000 IU/ml IFN-α or IFN-γ followed by the extraction of mRNA at different time points (0, 2, 5, 18, 24, 48, 72, and 96 h); in all cases, IFN-containing medium was removed after 5 h of stimulation. Expression of some of the most strongly up-regulated genes, including *CXCL9–11*, *GBP-1*, and *TRAIL*, was analyzed by quantitative PCR analysis, and results are illustrated in Fig. 2. The most striking finding was the different kinetics of the transcriptional up-regulation induced by type I and type II IFN in HUVEC. A marked increase in the expression of all these genes was noticed already after 2 h of stimulation in both IFN-α- and IFN-γ-stimulated HUVEC and peaked in most cases at 5 h after stimulation. In contrast, in the case of IFN-α stimulation the ex-pression of all genes analyzed substantially returned to baseline

levels by 18 h, whereas it remained persistently up-regulated after stimulation with IFN-γ, up to 96 h after stimulation in the case of GBP-1 and TRAIL transcripts.

Effects of IFN-α and IFN-γ stimulation on gene expression in various EC types

We next addressed the effect of IFN-α and IFN-γ on the expres-sion profile of *CXCL10*, *CXCL11*, and other selected genes in dif-ferent types of normal human EC, including two isolates of mi-crovascular cells (HMVEC no.1 and no.2) and HMVAR by both microarray and real-time PCR analysis. Comparison of the tran-scriptional responses to IFN-α treatment of HUVEC and HMVEC by microarrays revealed very similar expression profiles; Fig. 3 shows a scatter plot of microarray gene expression values of IFN-α-induced genes in the two EC types. Data were confirmed by real-time PCR of selected genes (Table VI); no major qualitative differences were observed for the different EC types as far as the direction of regulation and the ratio between IFN-α and IFN-γ were concerned. The only exceptions were *CXCL9*, which was much more strongly induced by IFN-γ in HMVEC and HMVAR than in HUVEC, and GBP-1, which was not induced in one of the

two HMVEC cell lines (Table VI). The preferential induction of *IFIT1*, *MX2*, and *OASL* by IFN-α observed for HUVEC (see Table III) was also confirmed for the other EC types examined (Table VI).

Expression of CXCL10, CXCL11 and TRAIL in the supernatant of IFN-stimulated EC

To confirm some of the more marked transcriptional changes at the protein level, we quantified by ELISA the levels of some chemokines in the supernatants of IFN-treated cells. CXCL10 was produced at low levels (range 0.1–0.7 ng/ml) by IFN-α-treated EC and at much higher levels following IFN-γ treatment (range 1–30 ng/ml); among EC, HMVARs produced the highest CXCL10 amounts (Fig. 4A). In contrast, HF released negligible levels of this cytokine in response to IFN-α, and only IFN-γ induced measurable CXCL10 production by these cells. Substantially similar findings were observed when we analyzed CXCL11 levels in the same samples. Following IFN-α treatment, CXCL11 was produced by all the different types of EC, but not by HF (Fig. 4A). Among the different EC types, however, some quantitative differences were evident, as CXCL11 levels were ~7-fold higher in HMVAR than in HMVEC. A much stronger difference emerged when IFN-α- and IFN-γ-treated cells were compared; 5–23 ng/ml CXCL11 was measured following IFN-γ treatment as compared with 0.02–0.6 ng/ml following IFN-α treatment (Fig. 4A). Finally, when TRAIL levels were measured, modest TRAIL release was observed in the supernatants of IFN-α- and IFN-γ-treated cells; in contrast, as recently observed for other cell types (30), treatment of EC with both cytokines was associated with a substantial increase in cell-associated TRAIL, whereas sizable TRAIL expression by HF was only induced by IFN-γ (Fig. 4B). To measure variations in protein levels over time, we treated HUVEC for 5 h with IFN-α or IFN-γ and then collected the conditioned medium at various time points and analyzed CXCL10 and CXCL11 concentrations by ELISA. Results are summarized in Fig. 4C. Following treatment with IFN-γ, CXCL10 and CXCL11 levels increased steadily during the 96-h interval. In contrast, following treatment with IFN-α, CXCL10 levels increased at early time points (18–48 h) but subsequently dropped at later time points (72–96 h). A modest increase in CXCL11 levels was measured during the same interval in IFN-α-treated HUVEC. Notably, at any given time point analyzed CXCL10 and CXCL11 levels were ~40- to 100-fold higher in supernatants of IFN-γ-treated HUVEC as compared with the corresponding IFN-α-treated cultures. A similar trend was also observed in kinetics experiments with HMVEC cells (data not shown). In general, the kinetics of CXCL10 and also partially CXCL11 protein expression were compatible with the transcriptional changes observed at the mRNA level.

Expression of CXCL10, CXCL11, and TRAIL in IFN-α-transduced xenografts

In view of the above data, which indicated that IFNs are able to up-regulate in vitro expression of some antiangiogenic chemokines by EC, we were interested in ascertaining whether a similar activity could also be recorded in vivo. Indeed, preliminary evidence (Fig. 5) showed that IFN-α was able to profoundly affect the pattern of chemokine expression by murine lung and dermal microvascular EC, as *CXCL10*, *CXCL11*, and *TRAIL* expressions were strongly up-regulated following in vitro treatment with murine rIFN-α (Fig. 5A). We thus wondered whether IFN-α could also affect in vivo the expression of some of the genes highlighted by the above analysis. To this end, we exploited a previously established xenotransplantation model based on parental or IFN-α-transduced MCF7 human breast cancer cells injected s.c. into SCID mice (4). As previously reported (4), the in vivo growth of
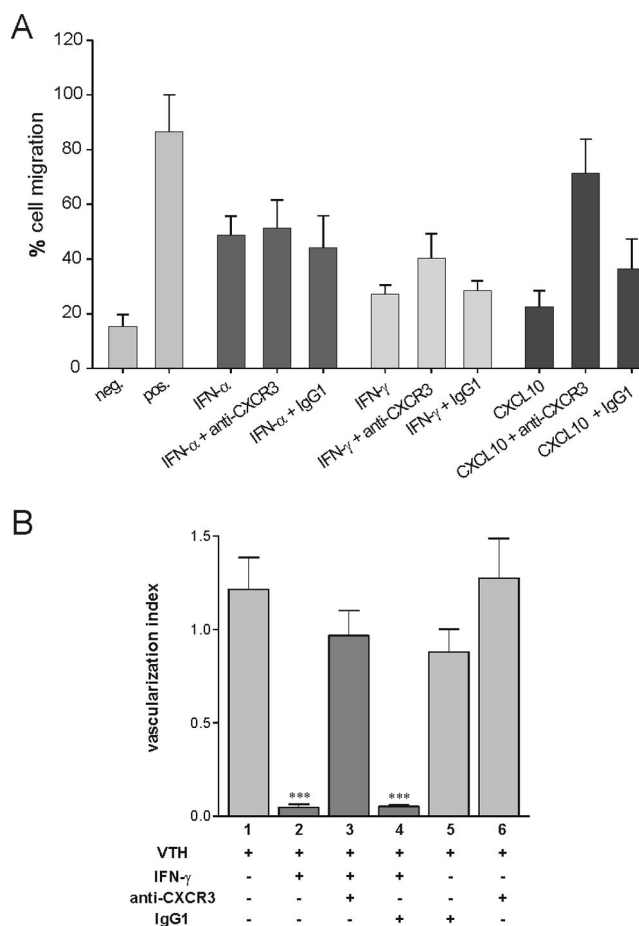

FIGURE 6. The antiangiogenic effects of IFN-γ are mediated by CXCR3, the receptor for CXCL10 and −11. *A,* Migratory response of HMVEC to conditioned medium from NIH 3T3 cells and the effects of IFN-α, IFN-γ and anti-CXCR3 Ab. An isotype-matched Ab (IgG1) was used to control the specificity of the anti-CXCR3 mAb. Migration was assessed using a modified Boyden chamber as described in *Materials and Methods.* neg., Negative; pos., positive. *B,* Matrigel pellets containing different combinations of VTH, IFN-γ, anti-CXCR3 mAb, and its isotype-matched control (as outlined at the *bottom* of the panel) were injected s.c. in C57BL/6 mice. Plugs were removed 6 days later and vascularization was measured in terms of hemoglobin content normalized over plug weight (vascularization index). Anti-CXCR3 Abs reversed the antiangiogenic effect of IFN-γ, whereas isotype-matched control Ab had no effect. The Abs alone in the absence of IFN-γ did not influence the vascularization of the plug.

IFN-α-producing tumors was greatly impaired compared with parental cells, and large areas of necrosis were present in IFN-α-expressing MCF7 tumors but not in control tumors (Fig. 5B). RT-PCR analysis of the RNA extracted from tumor tissues disclosed that *CXCL10*, *CXCL11*, and *TRAIL* transcription was dramatically up-regulated in IFN-α-expressing tumors as compared with control tumors (Fig. 5C). To identify which cells within the tumors were actually releasing CXCL11, we performed immunohistochemical analysis of MCF7 tumors. Although relatively few blood vessels could be analyzed because of the marked reduction in microvessel density in IFN-α-expressing tumor samples, CXCL11-producing cells were uniquely found in IFN-α-producing tumors and CXCL11 was predominantly expressed by EC within mid-size vessels (Fig. 5D). Among the other genes increased by IFN-α treatment of EC in vitro, GBP-1 expression was also dramatically increased in IFN-α-expressing tumors as compared with control tumors, both at the mRNA (not shown) and the protein level (Fig.

5E). Because both MCF7 and MCF7/IFN-α tumor cells only barely expressed GBP-1 (Fig. 5*E*), it is conceivable that GBP-1 in MCF7/IFN-α tumors was mainly produced by stromal cells under the influence of IFN-α. Unfortunately, the poor performance of the anti-GBP-1 Ab in immunohistochemistry assays precluded the possibility of further investigating the cellular source of GBP-1 in these samples.

CXCR-3 neutralization impairs but does not abrogate the antiangiogenic effects of IFNs

To analyze the functional role exerted by CXCL10 and CXCL11 in the antiangiogenic activity of IFNs, we performed an in vitro EC migration assay. As shown in Fig. 6*A*, EC migration was partially inhibited by both IFN-α and IFN-γ, albeit more markedly by the latter. Neutralization of CXCR3 partially restored the migration of IFN-γ-treated EC, whereas it had minimal effects on IFN-α-treated cells. In contrast, CXCL10 inhibited EC migration similarly to IFN-γ, and its effects were virtually blocked by anti-CXCR3 as expected. Altogether, these findings indicated that although both IFN-α and IFN-γ impaired EC migration in vitro, CXCR3-binding chemokines contributed mainly to the negative modulation of EC chemotaxis by IFN-γ.

To investigate whether this may also occur in vivo, Matrigel pellets containing the angiogenic mixture VTH and VTH plus IFN-γ with or without a neutralizing Ab to murine CXCR3 were injected under the skin of C57BL/6 mice. Four days later, Matrigel plugs were removed and vascularization measured in terms of hemoglobin content normalized over plug weight. As shown in Fig. 6*B*, anti-CXCR3 Ab reversed almost completely the antiangiogenic effects of IFN-γ, whereas control Abs did not. In conclusion, these results indicate that CXCR3 ligands substantially contribute to the antiangiogenic activity of IFN-γ.

Discussion

IFNs are known inducers of transcriptional changes, and their effects on the transcriptome of several cell types have been investigated in a number of studies (12, 15–18). The transcriptional effects of these cytokines on EC, however, have been only partially addressed (31) despite the broad evidence for their antiangiogenic effects (32–34). The aim of this work was to compare the in vitro effects of type I and type II IFNs on the transcriptional profile of EC of different origins and sources. We found that IFN effects are largely positive; hundreds of genes were up-regulated in EC, whereas we did not find any gene consistently down-regulated by IFN treatment. This finding partially contrasts with the observations by Taylor et al. (16), who analyzed the transcriptional effects in PBMC treated for 24 h with polyethylene glycol/IFN-α and observed that 534 genes were down-regulated, including genes associated with metabolism, macromolecule biosynthesis, and transcriptional regulation. Conceivably, differences in the cell types analyzed and the kinetics of treatment, as well as in the stringency of the bioinformatics parameters used, may explain these differences.

Class I IFNs comprise both IFN-α and IFN-β, which share a common receptor. It has been proposed that these two cytokines may activate receptors possessing distinct signaling properties and thus induce partially different transcriptional changes (10, 11). In our study, however, IFN-α and IFN-β elicited in HUVEC virtually identical transcriptional changes, thus reinforcing the conclusions obtained by da Silva et al. (35) by nonarray-based expression profiling. In contrast, many more pronounced differences were observed when the transcriptional changes induced in EC by IFN-α and IFN-γ were compared (see Table IV); as partly expected, genes involved in antiviral responses, such as viperin, *Mx1-2*,

IFIT1-1, and *OAS1-2*, were much more strongly up-regulated by class I than by class II IFN. Interestingly, many of these genes have been found to be induced by IFN-α but not by IFN-γ in the human fibrosarcoma cell line HT1080 (12). Overall, these findings likely reflect the fact that IFN-γ is induced as a part of the adaptive immune response to a wide variety of stimuli and is less strictly involved in the direct control of viral infections (36).

One major aim of this study was to identify genes that may contribute to explaining the angiostatic activity of IFN-α. Indeed, CXCL10 and CXCL11, whose expression was highly induced by IFN-α in EC but not in HF, could be very reasonable candidates for mediating this activity. In fact, much evidence indicates that CXC chemokines are involved in negative regulation of angiogenesis (reviewed in Ref. 37). In humans, CXCL9–11 exert their angiostatic activity through interaction with CXCR3-B, an alternatively spliced variant of the CXCR3 receptor selectively expressed by some types of EC during the S phase of the cell cycle (38), as well as by EC within tumors (39). We also confirmed *CXCR3-B* expression in HMVEC cultures by RT-PCR and flow cytometric analysis (data not shown). Notably, however, in our experimental system CXCR3 neutralization attenuated the negative modulation of EC chemotaxis by IFN-γ in vitro, whereas it did not affect IFN-α-mediated effects (Fig. 6*A*), possibly due to the profoundly different amounts of CXCL10 and CXCL11 produced by IFN-γ-stimulated EC as compared with IFN-α-stimulated EC (Fig. 4). The results of the in vivo angiogenesis assay also indicated that CXCR3 and its ligands mediate large part of the antiangiogenic effects of IFN-γ. In contrast, the finding that CXCR3 neutralization did not counteract the effects of IFN-α on EC migration may suggest that its angiostatic activity could possibly involve other pathways.

In this regard, among the genes induced at much higher levels in EC than in HF we found several genes involved in apoptosis, including TRAIL, a member of the TNF superfamily, and caspase 1 and 10. TRAIL, although generally associated with the induction of apoptosis in transformed cells, has been reported to exert heterogeneous effects in vitro on EC, depending on the phosphorylation status of Akt (40, 41). In our experimental system, IFN-α treatment of serum-deprived HUVEC elicited TRAIL production without increasing EC apoptosis, as measured by annexin V staining (data not shown); this could be likely due to the fact that TRAIL levels measured in EC following stimulation with IFN-α or IFN-γ were ~20-fold lower compared with those shown to be able to induce EC apoptosis in other experimental models (39). For the same reason, the contribution of TRAIL to the antiangiogenic effect of IFNs remains unclear. In fact, in vivo rTRAIL administration at concentrations far higher (250 ng/ml) than those obtained following treatment of EC with IFN (see Fig. 3) was able to reduce by 75% angiogenesis induced by a Kaposi's sarcoma-conditioned medium in a matrigel assay (data not shown). Although these observations indicate that TRAIL has indeed angiostatic activity, whether IFN-induced release of TRAIL by EC could play any role in a physiological setting merits further investigation.

A final family of genes that could conceivably contribute to the angiostatic effects of IFN-α is represented by GBPs. GBP-1 is among the major IFN-γ-induced proteins in human cells (42), and it has been shown to mediate antiviral effects against vesicular stomatitis and encephalomyocarditis viruses (43). Recently, it has been shown that these genes are induced in EC by various inflammatory cytokines, including IFNs (44), and could mediate inhibition of EC proliferation (45) and invasion (46). GBP-1 expression in EC has been documented in inflammatory skin disorders (47). Our microarray-based analysis confirms these findings (42, 44) and

indicates that *GBP-1* and *GBP-2* are among the genes preferentially activated by IFN-α in EC. Moreover, Western blot analysis clearly showed that GBP-1 is overexpressed in IFN-α-producing MCF7 tumors (Fig. 5*E*); as MCF7-IFN-α cells did not produce GBP-1, it is conceivable that GBP-1 was expressed by components of the tumor stroma. Ongoing studies are aimed at elucidating whether EC also contribute, as suggested by our in vitro studies, to GBP-1 production in these tumors and its contribution to the antiangiogenic activity of class I IFNs.

Notably, the most relevant transcriptional changes were confirmed at the protein level. In this respect, we observed a dramatic difference (~100-fold) between the amount of CXCL10 and CXCL11 in the supernatants of IFN-γ-treated EC compared with IFN-α-treated EC. Intriguingly, this was much less apparent when mRNA expression was measured, as *CXCL10* and *CXCL11* mRNA levels were only slightly higher in IFN-γ-treated than in IFN-α-treated HUVEC (see Fig. 1*B*). However, transcriptional changes in CXCL10 and CXCL11 levels induced by IFN-γ lasted much longer than those induced by IFN-α in EC, as shown by time course quantitative PCR analysis (Fig. 2). This surprising phenomenon, whose mechanism is currently unknown, may contribute to determine the markedly different amounts of chemokines produced by EC under the influence of IFN-α or IFN-γ.

CXCL11, a chemokine that has recently been associated with negative regulation of angiogenesis (48) and whose expression appears to be induced in vitro by IFN-α in an EC-specific fashion, was also shown to be produced in vivo by blood vessels located within IFN-α-expressing tumors; in general, CXCL11 expression was limited to mid-sized vessels, while most of the capillaries and postcapillary venules were not stained. It is currently unclear whether this may actually reflect in vivo production of higher amounts of this chemokine by EC from larger vessels as we observed in vitro in the case of HMVAR (see Fig. 4); alternatively, this finding could be due to poor sensitivity of the immunohistochemical technique used.

In any case, the finding that in a tumor model IFN-α elicits the expression of CXCL10 and CXCL11 emphasizes its complex role as an inhibitor of angiogenesis that, in addition to its established suppressive effects on the production of angiogenic factors by tumor cells (5–7), acts by up-regulating expression of antiangiogenic genes and by direct modulation of certain EC functions.

In conclusion, this study highlights the complex transcriptional signature of IFN in EC; although the great majority of the genes induced by IFN is substantially similar in EC, HF, and other cell types previously analyzed (16–18), it is interesting to observe that the magnitude of the transcriptional activation of the single genes may remarkably differ among different cell types. This agrees with findings by Schlaak et al. (17), who recently reported on cell type-specific IFN-α responses in various human cell lines using a restricted set of probes. Taken together, the data provide novel insights into the composition and function of the IFN-regulated transcriptome.

Disclosures

The authors have no financial conflict of interest.

References

1. Sidky, Y. A., and E. C. Borden. 1987. Inhibition of angiogenesis by interferons: effects on tumor- and lymphocyte-induced vascular responses. *Cancer Res.* 47: 5155–5161.
2. Rozera, C., D. Carlei, P. L. Lollini, C. De Giovanni, P. Musiani, E. Di Carlo, F. Belardelli, and M. Ferrantini. 1999. Interferon (IFN)-β gene transfer into TS/A adenocarcinoma cells and comparison with IFN-α: differential effects on tumorigenicity and host response. *Am. J. Pathol.* 154: 1211–1222.
3. Albini, A., C. Marchisone, F. Del Grosso, R. Benelli, L. Masiello, C. Tacchetti, M. Bono, M. Ferrantini, C. Rozera, M. Truini, et al. 2000. Inhibition of angiogenesis and vascular tumor growth by interferon-producing cells: a gene therapy approach. *Am. J. Pathol.* 156: 1381–1393.
4. Indraccolo, S., E. Gola, A. Rosato, S. Minuzzo, W. Habeler, V. Tisato, V. Roni, G. Esposito, M. Morini, A. Albini, et al. 2002. Differential effects of angiostatin, endostatin and interferon-α(1) gene transfer on in vivo growth of human breast cancer cells. *Gene Ther.* 9: 867–878.
5. Singh, R. K., M. Gutman, C. D. Bucana, R. Sanchez, N. Llansa, and I. J. Fidler. 1995. Interferons α and β down-regulate the expression of basic fibroblast growth factor in human carcinomas. *Proc. Natl. Acad. Sci. USA* 92: 4562–4566.
6. Oliveira, I. C., N. Mukaida, K. Matsushima, and J. Vilcek. 1994. Transcriptional inhibition of the interleukin-8 gene by interferon is mediated by the NF-κB site. *Mol. Cell. Biol.* 14: 5300–5308.
7. von Marschall, Z., A. Scholz, T. Cramer, G. Schafer, M. Schirner, K. Oberg, B. Wiedenmann, M. Hocker, and S. Rosewicz. 2003. Effects of interferon α on vascular endothelial growth factor gene transcription and tumor angiogenesis. *J. Natl. Cancer Inst.* 95: 437–448.
8. De Bouard, S., J. S. Guillamo, C. Christov, N. Lefevre, P. Brugieres, E. Gola, P. Devanz, S. Indraccolo, and M. Peschanski. 2003. Antiangiogenic therapy against experimental glioblastoma using genetically engineered cells producing interferon-α, angiostatin, or endostatin. *Hum. Gene Ther.* 14: 883–895.
9. Friesel, R., A. Komoriya, and T. Maciag. 1987. Inhibition of endothelial cell proliferation by γ-interferon. *J. Cell Biol.* 104: 689–696.
10. Angiolillo, A. L., C. Sgadari, D. D. Taub, F. Liao, J. M. Farber, S. Maheshwari, H. K. Kleinman, G. H. Reaman, and G. Tosato. 1995. Human interferon-inducible protein 10 is a potent inhibitor of angiogenesis in vivo. *J. Exp. Med.* 182: 155–162.
11. Sgadari, C., A. L. Angiolillo, B. W. Cherney, S. E. Pike, J. M. Farber, L. G. Koniaris, P. Vanguri, P. R. Burd, N. Sheikh, G. Gupta, et al. 1996. Interferon-inducible protein-10 identified as a mediator of tumor necrosis in vivo. *Proc. Natl. Acad. Sci. USA* 93: 13791–13796.
12. Der, S. D., A. Zhou, B. R. Williams, and R. H. Silverman. 1998. Identification of genes differentially regulated by interferon α, β, or γ using oligonucleotide arrays. *Proc. Natl. Acad. Sci. USA* 95: 15623–15628.
13. Krepler, C., U. Certa, V. Wacheck, B. Jansen, K. Wolff, and H. Pehamberger. 2004. Pegylated and conventional interferon-α induce comparable transcriptional responses and inhibition of tumor growth in a human melanoma SCID mouse xenotransplantation model. *J. Invest. Dermatol.* 123: 664–669.
14. Tracey, L., I. Spiteri, P. Ortiz, M. Lawler, M. A. Piris, and R. Villuendas. 2004. Transcriptional response of T cells to IFN-α: changes induced in IFN-α-sensitive and resistant cutaneous T cell lymphoma. *J. Interferon Cytokine Res.* 24: 185–195.
15. Ji, X., R. Cheung, S. Cooper, Q. Li, H. B. Greenberg, and X. S. He. 2003. Interferon α regulated gene expression in patients initiating interferon treatment for chronic hepatitis C. *Hepatology* 37: 610–621.
16. Taylor, M. W., W. M. Grosse, J. E. Schaley, C. Sanda, X. Wu, S. C. Chien, F. Smith, T. G. Wu, M. Stephens, M. W. Ferris, et al. 2004. Global effect of PEG-IFN-α and ribavirin on gene expression in PBMC in vitro. *J. Interferon Cytokine Res.* 24: 107–118.
17. Schlaak, J. F., C. M. Hilkens, A. P. Costa-Pereira, B. Strobl, F. Aberger, A. M. Frischauf, and I. M. Kerr. 2002. Cell-type and donor-specific transcriptional responses to interferon-α. Use of customized gene arrays. *J. Biol. Chem.* 277: 49428–49437.
18. de Veer, M. J., M. Holko, M. Frevel, E. Walker, S. Der, J. M. Paranjape, R. H. Silverman, and B. R. Williams. 2001. Functional classification of interferon-stimulated genes identified using microarrays. *J. Leukocyte Biol.* 69: 912–920.
19. Roni, V., W. Habeler, A. Parenti, S. Indraccolo, E. Gola, V. Tosello, R. Cortivo, G. Abatangelo, L. Chieco-Bianchi, and A. Amadori. 2003. Recruitment of human umbilical vein endothelial cells and human primary fibroblasts into experimental tumors growing in SCID mice. *Exp. Cell Res.* 287: 28–38.
20. Irizarry, R. A., B. M. Bolstad, F. Collin, L. M. Cope, B. Hobbs, and T. P. Speed. 2003. Summaries of Affymetrix gene chip probe level data. *Nucleic Acids Res.* 31: e15.
21. Zhang, J., V. Carey, and R. Gentleman. 2003. An extensible application for assembling annotation for genomic data. *Bioinformatics* 19: 155–156.
22. Tusher, V. G., R. Tibshirani, and G. Chu. 2001. Significance analysis of microarrays applied to the ionizing radiation response. *Proc. Natl. Acad. Sci. USA* 98: 5116–5121.
23. Dennis, G., Jr., B. T. Sherman, D. A. Hosack, J. Yang, W. Gao, H. C. Lane, and R. A. Lempicki. 2003. DAVID: Database for annotation, visualization, and integrated discovery. *Genome Biol.* 4: P3.
24. Rosen, S. and H. J. Skaletsky. 2000. Primer3 on the WWW for general users and for biologist programmers. In *Bioinformatics Methods and Protocols: Methods in Molecular Biology.* S. Misener and S. A. Krawetz, eds. Humana Press, Totowa, NJ, p. 365–386.
25. Muller, P. Y., H. Janovjak, A. R. Miserez, and Z. Dobbie. 2002. Processing of gene expression data generated by quantitative real-time RT-PCR. *BioTechniques* 32: 1372–1379.

26. Albini, A., G. Fontanini, L. Masiello, C. Tacchetti, D. Bigini, P. Luzzi, D. M. Noonan, and W. G. Stetler-Stevenson. 1994. Angiogenic potential in vivo by Kaposi's sarcoma cell-free supernatants and HIV-1 tat product: inhibition of KS-like lesions by tissue inhibitor of metalloproteinase-2. *AIDS* 8: 1237–1244.

27. Chin, K. C., and P. Cresswell. 2001. Viperin (cig5), an IFN-inducible antiviral protein directly induced by human cytomegalovirus. *Proc. Natl. Acad. Sci. USA* 98: 15125–15130.

28. Bluyssen, H. A., R. J. Vlietstra, P. W. Faber, E. M. Smit, A. Hagemeijer, and J. Trapman. 1994. Structure, chromosome localization, and regulation of expression of the interferon-regulated mouse Ifi54/Ifi56 gene family. *Genomics* 24: 137–148.

29. Strieter, R. M., J. A. Belperio, R. J. Phillips, and M. P. Keane. 2004. CXC chemokines in angiogenesis of cancer. *Semin. Cancer Biol.* 14: 195–200.

30. Cassatella, M. A., V. Huber, F. Calzetti, D. Margotto, N. Tamassia, G. Peri, A. Mantovani, L. Rivoltini, and C. Tecchio. 2005. Interferon-activated neutrophils store a TNF-related apoptosis-inducing ligand (TRAIL/Apo-2 ligand) intracellular pool that is readily mobilizable following exposure to proinflammatory mediators. *J. Leukocyte Biol.* 79: 123–132.

31. Sana, T. R., M. J. Janatpour, M. Sathe, L. M. McEvoy, and T. K. McClanahan. 2005. Microarray analysis of primary endothelial cells challenged with different inflammatory and immune cytokines. *Cytokine* 29: 256–269.

32. Kerbel, R., and J. Folkman. 2002. Clinical translation of angiogenesis inhibitors. *Nat. Rev. Cancer* 2: 727–739.

33. Marler, J. J., J. B. Rubin, N. S. Trede, S. Connors, H. Grier, J. Upton, J. B. Mulliken, and J. Folkman. 2002. Successful antiangiogenic therapy of giant cell angioblastoma with interferon α 2b: report of 2 cases. *Pediatrics* 109: E37.

34. Chang, E., A. Boyd, C. C. Nelson, D. Crowley, T. Law, K. M. Keough, J. Folkman, R. A. Ezekowitz, and V. P. Castle. 1997. Successful treatment of infantile hemangiomas with interferon-α-2b. *J. Pediatr. Hematol. Oncol.* 19: 237–244.

35. da Silva, A. J., M. Brickelmaier, G. R. Majeau, A. V. Lukashin, J. Peyman, A. Whitty, and P. S. Hochman. 2002. Comparison of gene expression patterns induced by treatment of human umbilical vein endothelial cells with IFN-α 2b vs. IFN-β 1a: understanding the functional relationship between distinct type I interferons that act through a common receptor. *J. Interferon Cytokine Res.* 22: 173–188.

36. Stark, G. R., I. M. Kerr, B. R. Williams, R. H. Silverman, and R. D. Schreiber. 1998. How cells respond to interferons. *Annu. Rev. Biochem.* 67: 227–264.

37. Romagnani, P., L. Lasagni, F. Annunziato, M. Serio, and S. Romagnani. 2004. CXC chemokines: the regulatory link between inflammation and angiogenesis. *Trends Immunol.* 25: 201–209.

38. Romagnani, P., F. Annunziato, L. Lasagni, E. Lazzeri, C. Beltrame, M. Francalanci, M. Uguccioni, G. Galli, L. Cosmi, L. Maurenzig, et al. 2001. Cell cycle-dependent expression of CXC chemokine receptor 3 by endothelial cells mediates angiostatic activity. *J. Clin. Invest.* 107: 53–63.

39. Lasagni, L., M. Francalanci, F. Annunziato, E. Lazzeri, S. Giannini, L. Cosmi, C. Sagrinati, B. Mazzinghi, C. Orlando, E. Maggi, et al. 2003. An alternatively spliced variant of CXCR3 mediates the inhibition of endothelial cell growth induced by IP-10, Mig, and I-TAC, and acts as functional receptor for platelet factor 4. *J. Exp. Med.* 197: 1537–1549.

40. Alladina, S. J., J. H. Song, S. T. Davidge, C. Hao, and A. S. Easton. 2005. TRAIL-induced apoptosis in human vascular endothelium is regulated by phosphatidylinositol 3-kinase/Akt through the short form of cellular FLIP and Bcl-2. *J. Vasc. Res.* 42: 337–347.

41. Secchiero, P., A. Gonelli, E. Carnevale, D. Milani, A. Pandolfi, D. Zella, and G. Zauli. 2003. TRAIL promotes the survival and proliferation of primary human vascular endothelial cells by activating the Akt and ERK pathways. *Circulation* 107: 2250–2256.

42. Cheng, Y. S., R. J. Colonno, and F. H. Yin. 1983. Interferon induction of fibroblast proteins with guanylate binding activity. *J. Biol. Chem.* 258: 7746–7750.

43. Anderson, S. L., J. M. Carton, J. Lou, L. Xing, and B. Y. Rubin. 1999. Interferon-induced guanylate binding protein-1 (GBP-1) mediates an antiviral effect against vesicular stomatitis virus and encephalomyocarditis virus. *Virology* 256: 8–14.

44. Naschberger, E., T. Werner, A. B. Vicente, E. Guenzi, K. Topolt, R. Leubert, C. Lubeseder-Martellato, P. J. Nelson, and M. Sturzl. 2004. Nuclear factor-κB motif and interferon-α-stimulated response element cooperate in the activation of guanylate-binding protein-1 expression by inflammatory cytokines in endothelial cells. *Biochem. J.* 379: 409–420.

45. Guenzi, E., K. Topolt, E. Cornali, C. Lubeseder-Martellato, A. Jorg, K. Matzen, C. Zietz, E. Kremmer, F. Nappi, M. Schwemmle, C. Hohenadl, et al. 2001. The helical domain of GBP-1 mediates the inhibition of endothelial cell proliferation by inflammatory cytokines. *EMBO J.* 20: 5568–5577.

46. Guenzi, E., K. Topolt, C. Lubeseder-Martellato, A. Jorg, E. Naschberger, R. Benelli, A. Albini, and M. Sturzl. 2003. The guanylate binding protein-1 GTPase controls the invasive and angiogenic capability of endothelial cells through inhibition of MMP-1 expression. *EMBO J.* 22: 3772–3782.

47. Lubeseder-Martellato, C., E. Guenzi, A. Jorg, K. Topolt, E. Naschberger, E. Kremmer, C. Zietz, E. Tschachler, P. Hutzler, M. Schwemmle, et al. 2002. Guanylate-binding protein-1 expression is selectively induced by inflammatory cytokines and is an activation marker of endothelial cells during inflammatory diseases. *Am. J. Pathol.* 161: 1749–1759.

48. Burdick, M. D., L. A. Murray, M. P. Keane, Y. Y. Xue, D. A. Zisman, J. A. Belperio, and R. M. Strieter. 2005. CXCL11 attenuates bleomycin-induced pulmonary fibrosis via inhibition of vascular remodeling. *Am. J. Respir. Crit. Care Med.* 171: 261–268.